ACS chemical biology

ARTICLES

pubs.acs.org/acschemicalbiology

Parsimonious Discovery of Synergistic Drug Combinations

Bryan Severyn, Robert A. Liehr, Alex Wolicki, Kevin H. Nguyen,[‡] Edward M. Hudak, Marc Ferrer,[§] Jeremy S. Caldwell,[†] Jeffrey D. Hermes, Jing Li, and Matthew Tudor*

Merck Research Laboratories, North Wales, Pennsylvania 19454, United States

[†]Merck Research Laboratories, West Point, Pennsylvania 19486, United States

Supporting Information

ABSTRACT: Combination therapies that enhance efficacy or permit reduced dosages to be administered have seen great success in a variety of therapeutic applications. More fundamentally, the discovery of epistatic pathway interactions not only informs pharmacologic intervention but can be used to better understand the underlying biological system. There is, however, no systematic and efficient method to identify interacting activities as candidates for combination therapy and, in particular, to identify those with synergistic activities. We devised a pooled, self-deconvoluting screening paradigm for the efficient comprehensive interrogation of all pairs of compounds in 1000-compound libraries. We demonstrate the power of the method to recover established synergistic interactions between compounds. We then applied this approach to a cell-based screen for anti-inflammatory activities using an assay for lipopolysaccharide/interferon-induced acute phase response of a monocytic cell line. The described method, which is >20 times as efficient as a naïve approach, was used to test all pairs of 1027 bioactive compounds for interleukin-6 suppression, yielding 11 pairs of compounds that show synergy. These 11 pairs all represent the same two activities: β-adrenergic receptor agonists and phosphodiesterase-4 inhibitors. These activities both act through cyclic AMP elevation and are known to be anti-inflammatory alone and to synergize in combination. Thus we show proof of concept for a robust, efficient technique for the identification of synergistic combinations. Such a tool can enable qualitatively new scales of pharmacological research and chemical genetics.

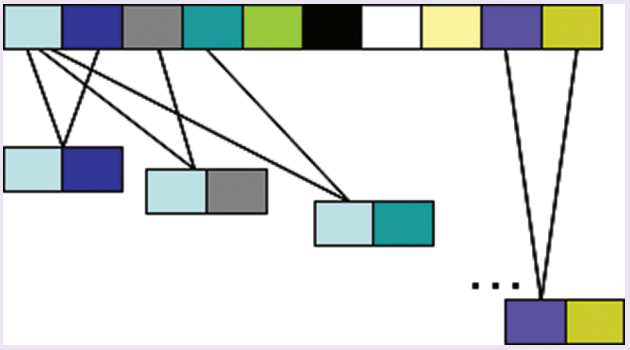

Combinations of pharmaceuticals have significant potential benefits over single agents as therapeutics.[1,2] Two areas where combinations are used routinely are antiinfectives[3,4] and cancer chemotherapeutics.[5] In these areas, high mutation rates and selection pressure favor emergence of resistant variants, and combinations are used to reduce the probability of resistance. In other therapeutic areas, combination treatments are used to enhance the effectiveness (*e.g.*, in COPD[6]) or reduce toxicities of (often chronic) treatments (*e.g.*, in burns[7] and immunosuppression[8,9]).

Synergistic combinations are of particular interest as they show enhanced activity of the mixture relative to that expected from additivity of the components' effects. Synergistic combinations that show increased potency (equivalent therapeutic effects are seen at lower doses) are of practical interest because they offer the highest dose reduction[10] and thus minimize toxicities. Another potentially beneficial mode of synergy is enhanced efficacy (whereby the combination has more therapeutic benefit than is attained by the single agents at any dose).

Traditionally, combination treatments are created by combining standard of care compounds in a hypothesis-driven manner. For example, two or more antibiotics targeting the same class of bacteria may be mixed,[11] or an antibiotic may be combined with a resistance inhibitor.[12] This method will not uncover unanticipated interactions between targets not thought to be mechanistically linked, and sometimes such rational designs may fail to be empirically confirmed.[13] An alternative approach to the problem of finding efficacious combinations is an unbiased combinatorial screen.[14] The problem with such approaches is their geometric scaling. Thus, testing all pairwise combinations of only 1000 compounds leads to $\sim 5 \times 10^5$ assays (combinations of 1000 items taken 2 at a time, ${}_{1000}C_2 = 1000!/(998!*2!) = 495{,}000$). Looked at another way, whereas a typical pharmaceutical screening library is on the order of 10^6 compounds, and screening capacity is scaled accordingly, 10^6 data points represents all pairs of only ~1400 compounds. Thus, an attempt to systematically test for combination effects rapidly exhausts screening capacity. Herein, we present a more efficient strategy to identify efficacious molecular partners.

RESULTS AND DISCUSSION

It has been observed that pooling of chemical libraries to reduce screen size can lead to undesirable false negative and false

Received: April 6, 2011
Accepted: October 5, 2011
Published: October 05, 2011

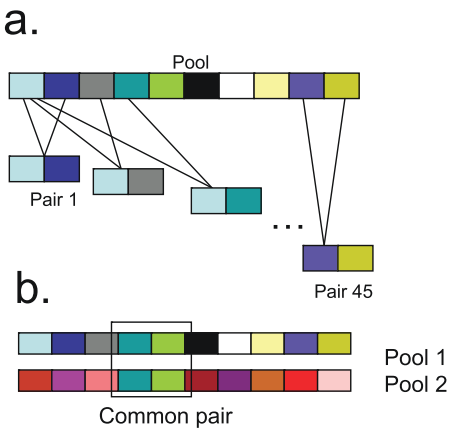

Figure 1. Design and execution of screen. (a) Illustration of the 45 pairs encompassed by a pool of 10 compounds, depicted as colored blocks. (b) Illustration of self-deconvoluting design whereby each pair is contained in two different pools of 10 compounds with otherwise distinct members. For a pair to be considered active, both pools must score in the phenotypic assay. In that case, the responsible pair can be identified as the only common one, thus obviating the need for retesting all 45 pairs in follow-up.

positive effects relative to unpooled screens.[15] We hypothesized that at least some of these artifactual findings are due to epistasis among compounds: sets of molecules whose activities on the cell either enhance or suppress each other. It was of interest to determine if we could take advantage of pooling to seek, rather than overcome, epistatic interactions. A pool of 10 compounds contains 45 pairs ($_{10}C_2$, Figure 1a), implying that a screen using pools of 10 compounds would be reduced in size by a factor of 45 relative to testing all pairwise interactions individually. In practice, it has been seen that traditional pooled screening followed by retesting of components of the active pools is an inefficient process since the second step is often larger in scale than the first. To surmount this obstacle, traditional pooled screening has used self-deconvoluting designs.[16] Such designs test each compound in at least two pools with otherwise different partners, then if two pools containing a compound show activity, it can be surmised that the one common component is active. Therefore, we applied a self-deconvoluting design to our combination screen by developing a library in which each *pair* of compounds is represented in multiple pools with otherwise distinct compounds (Figure 1b). Finally, to facilitate analysis, each compound is tested alone as well as in pools.

There are several assumptions that must be met for this approach to be effective: first, synergy must be rare (otherwise too many pools would be active and deconvolution would be impossible). Next, the dose used must be amenable (if a potentiation exists between two compounds, the doses of both must elicit a submaximal response). Third, the screening assay must be robust, as a high false negative rate will interfere with deconvolution. We have seen that even in compound libraries that are enriched for bioactives, synergistic interactions are rare (<2% of pairs, see below). Whereas the described method uses constant compound concentrations (1 μM in primary screen), an obvious extension is to first establish single-compound dose responses and then use active singles at an EC_{10} (a concentration eliciting 10% of maximal response). We find that a 1536-well platform is ideally suited for this scale of experiment, and many relevant assays have been miniaturized to perform robustly in this format.[17,18]

In order to assess the ability of our pooled synergy screening approach to recover known synergistic interactions, we first empirically identified synergistic interactions using the traditional approach of matrixed dose−response analysis. We performed a viability assay in a commonly used colorectal cancer cell line, HCT116, using 11 oncological chemotherapeutics with diverse targets (Supplementary Table 1, items 1−11). The compounds were tested in eight-point dose−response assays in all pairwise combinations (55 pairs), and synergy was assessed by various metrics.

There exist several methods for characterizing interactions between compounds,[19] and we briefly describe three approaches we have found useful. Traditional isobologram methods are based on Loewe additivity,[20] which assumes the two compounds have the same target and is quantified by the Combination Index.[10] Synergy is modeled on the basis of the ability of the combination to achieve activity at lower concentrations of the constituents than would be expected from their additive effects. Bliss independence[21] can be used to model activities with different targets. This models a noninteraction as multiplicative of its constituent fractional activities.[22] Finally, the highest single activity ("highest single agent"[14]) approach looks for activity beyond that of the most active component. This is not a synergy model as such, capturing additivity as well as synergy, but is a useful heuristic that is less conservative than the alternatives. For pooled screens, all of these metrics were adapted to multicompound combinations rather than the traditional pairwise calculations.

We analyzed the matrixed dose responses of HCT116 cell viability with all three of the above methods and settled on the Bliss independence criterion as a means of selecting actives. This decision was made in part because the targets of the compounds in question are known to be different (*i.e.*, the compounds are mutually nonexclusive inhibitors) and in part because the Bliss model is more stringent than the HSA criterion in discounting additive interactions. Figure 2a presents the results of the synergy analysis using the Bliss model for compound independence. We set a conservative threshold to define strongly synergistic compound pairs (>20% excess activity over the Bliss model at more than one dose of each compound, seen reproducibly with replicate Z scores >4). A more inclusive threshold was used to identify moderate evidence for synergy (>20% excess activity over Bliss model for at least one dose combination). Significantly, synergies between several of these pairs of activities have been previously reported, including interactions between MEK and PI3K inhibitors,[23,24] MEK and EGFR inhibitors,[25] MEK inhibitors and the multikinase inhibitor sorafenib,[26] and the multikinase inhibitor dasatinib with HSP90 inhibitors.[27]

We next used the 11 compounds ("query compounds") in the background of 89 other compounds selected for diversity from a commercial compound collection. The 100 compounds (Supplementary Table 1) were tested in the pooled synergy screening paradigm to assess empirical operating characteristics for the approach. The 4950 pairs of 100 compounds were screened in 136 pools of 10 compounds each, at a final compound concentration of 1 μM. To permit unique deconvolution of the pairs in positive pools, the 136-pool design was repeated four times with different compound permutations. Finally, the individual compounds were tested alone in duplicate as well. The full experiment consisted of one-half of a 1536-well plate (768 wells, including controls) and was performed in duplicate.

The viability readings of the duplicate experiments were highly reproducible (R^2 ~0.98). We calculated synergy metrics based

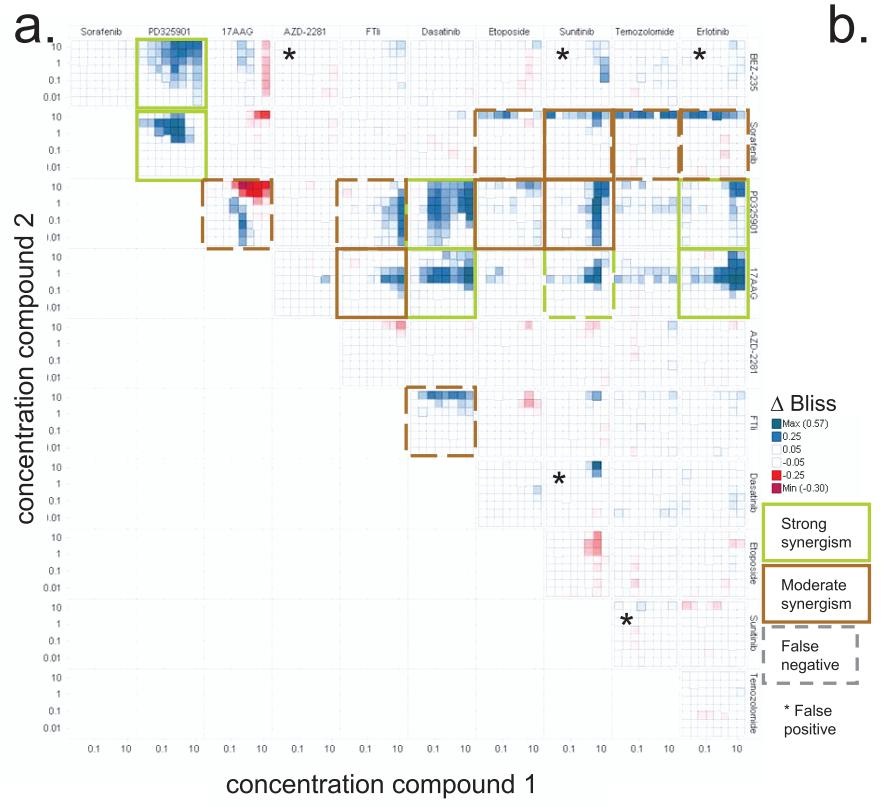

b.

	component 1	component 2
1	Etoposide	PD325901
2	PD325901	Sorafenib
3	BEZ-235	AZD-2281
4	FTI inhibitor	17-AAG
5	17-AAG	Erlotinib
6	PD325901	Erlotinib
7	BEZ-235	Erlotinib
8	Sunitinib	PD325901
9	BEZ-235	Sunitinib
10	Dasatinib	17-AAG
11	Dasatinib	PD325901
12	BEZ-235	PD325901
13	Sunitinib	Sorafenib
14	Sunitinib	Temozolomide
15	Dasatinib	Sunitinib

Figure 2. (a) HCT116 viability screen results. ΔBliss values (difference between observed and expected results under Bliss independence) are depicted in a heat map with subplots for individual pairs of compounds. Positive values (blue) indicate inhibition of cell growth higher than expected on the basis of the single compound effects at the given dose. Pairs showing strong synergism are boxed in green, and moderate synergism is boxed in brown. False negatives in the pooled screen are indicated as dashed boxes, and false positives in the pooled screen are indicated with asterisks. (b) Pairs of query compounds that were positive in the pooled screen. Green-shaded pairs were previously established (panel a) to be strongly synergistic, brown-shaded pairs were moderately synergistic, while white pairs were not considered synergistic in the pairwise matrixed dose−response analysis.

on Bliss,[21] HSA,[14] and Loewe[10] models and selected hits based on departure from the noninteraction expectations of the various models. On the basis of exploratory analysis of the data, we settled on a synergism threshold of >10% excess activity over that expected by both Bliss and HSA models, yielding 53 hit pools (Supplementary Figure 1).

To deconvolute the active pairs of compounds in the 10-compound pools, the hit wells were analyzed for common pairs of compounds. We found 81 pairs that could be unambiguously identified as active because they appeared at least three times in the 53 hit pools. These 81 pairs are designated synergistic interactants based on the pooled screen, and this list can be compared to our previously established classification of strongly, moderately, and nonsynergistic pairs (Figure 2a). Of 81 pairs, 15 were synergies between two query compounds, and we used these to assess false positive and negative rates of the methodology (Figure 2b). The pooled synergy screening approach recovered 6/7 of our previously defined strongly synergistic compound pairs (false negative rate of 14%) and 4/10 of moderately synergistic combinations (false negative rate 60%). Additionally, the pooled screen identified as synergistic 5 of the 38 pairs that did not show significant synergism in the matrixed dose−response analysis, implying a false positive rate of 13% (Supplementary Figure 1). The false positive rate is of less concern because, as demonstrated below, false positives can be triaged in follow-up experiments. However, false negatives represent lost opportunities and are therefore important to minimize. Our pooled synergy screening approach demonstrates a relatively high sensitivity to uncover synergistic interactions.

In order to test a larger compound set using more specific biology, we next implemented a screen for anti-inflammatory combinations. The THP-1 monocytic cell line was stimulated with a pro-inflammatory cocktail (lipopolysaccharide plus interferon γ), and compounds that synergistically inhibit the acute phase response, as read out by IL6 secretion, were identified; 1027 compounds were tested for their ability to interfere with the IL6 response, both alone and in pooled combinations. Using this pooled, self-deconvoluting design, we reduced the size of the screen from $\sim 10^6$ wells (for duplicated all-pairs assay), to 31,236 wells, a scale that can be easily screened without the need for robotics (22 × 1536-well plates including controls). No absolute hit threshold was established on the raw signal or percent inhibition, but rather hits were chosen on the basis of the departure of the individual well's signal from that expected under independence or additivity of the compounds (Figure 3a). Potential actives were identified on the basis of the union of the three described synergy metrics (*i.e.*, pairs were followed up if they passed a threshold on any of the tests for synergy).

From the primary screen, 350 hit pools were identified, and in deconvolution these pools yielded 228 pairs that replicated (assuming independent distribution of pairs among 350 pools,

dx.doi.org/10.1021/cb2003225 |*ACS Chem. Biol.* 2011, 6, 1391–1398

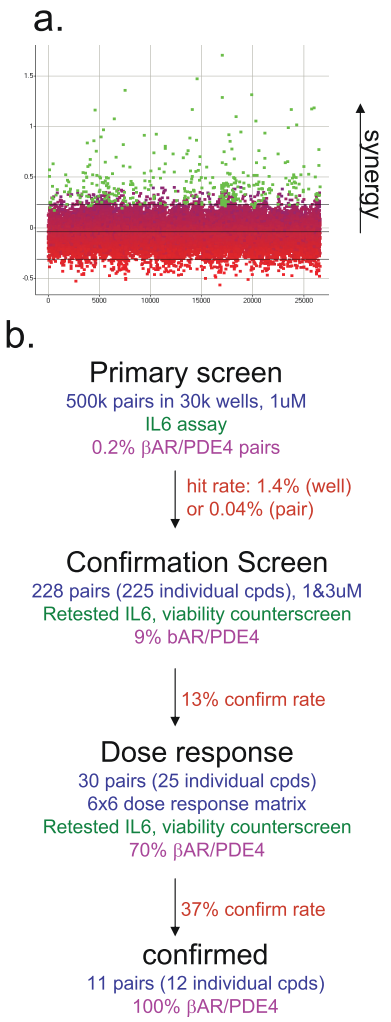

Figure 3. (a) Depiction of ΔHSA synergy metric, versus run order in the inflammation screening campaign. Based on the single-compound treatments, the maximal activity of the component compounds of each pool is calculated. Departures from this highest single activity (ΔHSA) in the positive direction suggest synergy, in the negative direction antagonism. The mean ± 2 standard deviations are shown as horizontal lines. Hits were selected on the basis of the HSA model (criterion: ΔHSA > 0.4, *i.e.*, 40% higher activity than predicted by most active single agent) as well as Bliss and Combination Index algorithms. The union of these hit lists is colored green in the plot. (b) Screen summary including hit and confirmation rates.

115 would be expected by chance, $p \sim 10^{-10}$, Fisher exact test). This hit rate represents 1.4% of the pools but only 0.04% of the pairs screened (Figure3 b).

We took these 228 pairs forward into confirmation. The confirmation phase tested the pairs individually in triplicate at two concentrations (1 and 3 μM), using the original IL6 inhibition assay and a viability control assay. Thirty (13%) of the pairs confirmed in the IL6 assay (Figure 3 b), and none of the pairs had significant reductions in viability at the time point tested (not shown). Interestingly, 21 of the 30 confirmed pairs consisted of the same two activities in combination: phosphodiesterase 4 (PDE4) inhibitors and β-adrenergic receptor (βAR) agonists. Given the prevalence of these two target classes in the starting library (10 compounds each), this represents a significant enrichment of the pair ($p < 10^{-15}$, Fisher exact test).

We can use the confirmation results to estimate the false negative rate of the screen based on the coverage of βAR and PDE4 compounds in the initial collection. Five out of 10 βAR and eight out of 10 PDE4 compounds were members of pairs that showed activity in the IL6 assay. One would expect all pairs of these to be active, yielding 40 pairs. Since 21 were recovered, this suggests a false negative rate of ~48%, in line with the measured false negative rate of 14−60% in the HCT116 viability assay. If screening collections are designed with at least two representative compounds for each target class, and given this false negative rate, there is a ~95% chance of identifying at least one of the pairs as active at this stage ($1-0.48^4$), suggesting that the pooled synergy screening approach can have high power to identify active combinations.

To validate the results, we then tested the confirmed 30 pairs in a dose−response assay. A 6 × 6 matrix dose response was constructed for each pair, and IL6 inhibition and viability were assayed. Figure 4 shows one example pair in this assay. It can be seen that the activity reached at the highest dose (14.3 μM) of each compound alone (lowest blue curves in Figure 4a,b, left column and bottom row of Figure 4c), is exceeded in all cases when the second compound is present at any dose. This is an efficacy boost in addition to a potentiation (leftward shift of dose curve; decreased EC_{50}), which is seen only for the second compound (Figure 4b). It can be seen that this efficacy boost is well captured as synergistic by two standard models of synergy: highest single activity (HSA) and the Bliss model (Figure 4d,e). In contrast, the combination index, which models only potency shifts, does not capture the synergy (Figure 4f). Also notable is the ability of the approach to robustly recover synergistic interaction in the presence of experimental noise (assay Z′ factor ~0.3;[28] see for example variability in Cpd02-only dose curve, lowest blue curve and circle markers, Figure 4a).

We conservatively considered pairs to be validated as synergistic combinations only if they showed synergism at more than one dose. Eleven out of the 30 pairs were validated; all of them were composed of one βAR agonist and one PDE4 inhibitor (Figure 3b, Table 1). Because 10 of the pairs targeting βAR and PDE4 did not validate, new analyses may need to be applied to decrease false negatives at the validation stage. Structures of the validated compounds are presented in Supplementary Table 2.

The combination of βAR agonists and PDE inhibitors elevates cAMP to levels unobtainable either in the absence of cAMP production (*i.e.*, without adrenergic activation) or in the presence of its hydrolysis (*i.e.*, without PDE inhibition). Both βAR agonism[29−31] and PDE4 antagonism[32,33] are independently known to be anti-inflammatory. Additionally, it has been reported that the combination of these two activities can act synergistically.[34−36] Thus, our findings are consistent with established biology and provide a proof-of-concept for the synergy screening platform.

The mode of synergy that we observe is an efficacy boost, whereby the maximal attenuation of IL6 activity was increased approximately 2-fold (Figure 4). In this case, one can hypothesize that this synergy is due to the fact that each activity independently leads to increased cAMP, with further increased levels resulting from the combination. This is distinct from potency shifts often seen with compounds affecting the same target or pathway and modeled with the combination index.[10] Under a Loewe model, each compound can fully inhibit the response, and the combination results in complete inhibition at lower doses than for each single agent. Therefore, the efficacy boost is best assessed using departures from a Bliss model[21] or excess over the

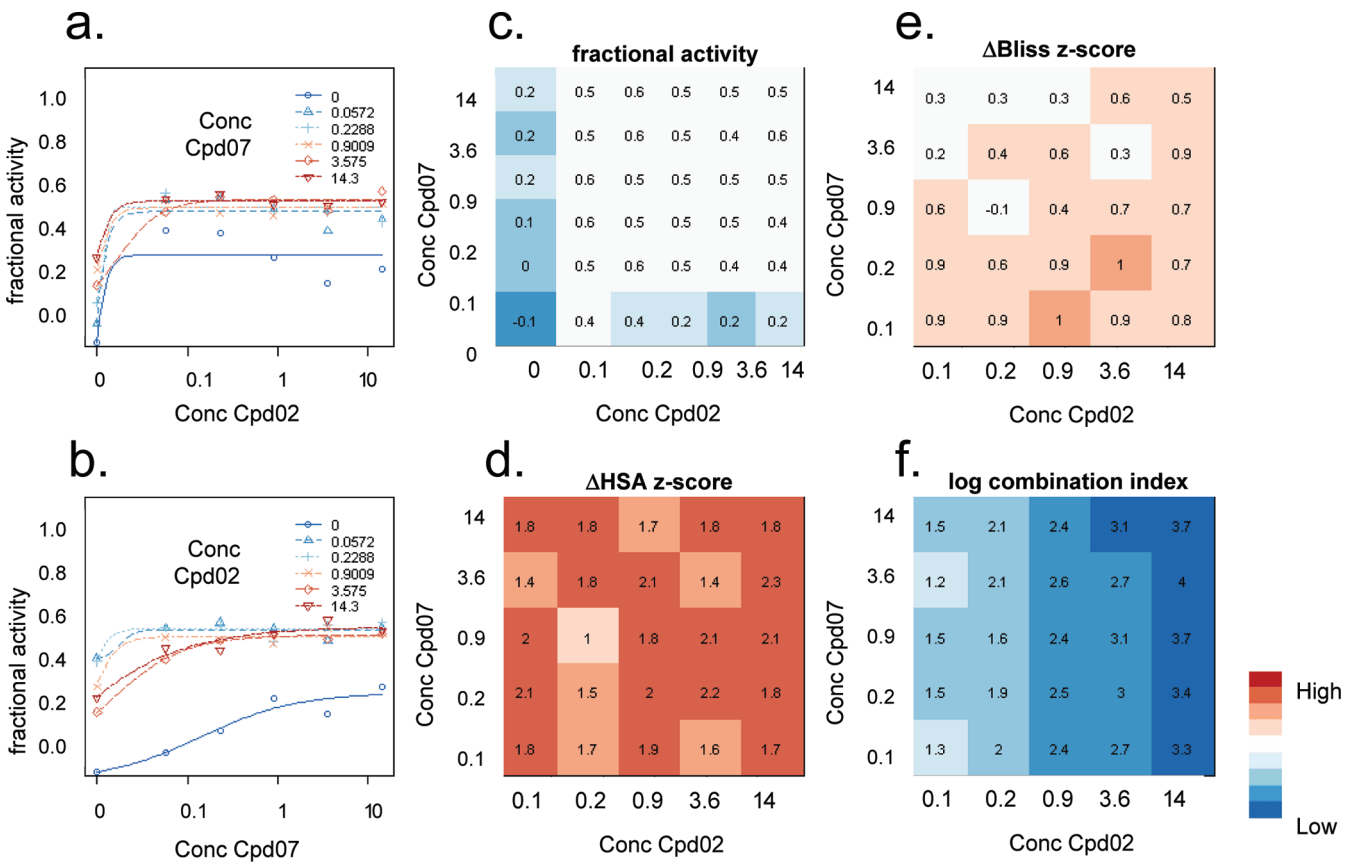

Figure 4. Dose−response analysis of one confirmed active pair from the inflammation screen. (a) Dose response of Cpd02 (horizontal axis, in μM) at different concentrations of Cpd07 (indicated by colors). Plotted against dose is the fractional activity (response scaled between 0, no inhibition, to 1, complete inhibition). (b) Cpd07 concentration on horizontal axis at different concentrations of Cpd02 (color key). (c) Heat map depicting same fractional activity data as panels a and b. Cpd02 is on the horizontal axis, and Cpd07 on the vertical axis. Color map: 0 (blue, no inhibition) to 1 (red, complete inhibition). (d) ΔHSA *z*-score heatmap showing departures from highest single activity synergy model, Color map: −3 (blue, antagonism) to 3 (red, synergy or additivity). (e) ΔBliss *z*-score heatmap showing departures from Bliss independence model. Color map: −3 (blue, antagonism) to 3 (red, synergy). (f) Departures from Loewe additivity model as calculated by $\log_{10}$ combination index. Color map: 4 (blue, antagonism) to −4 (red, synergy).

Table 1. Validated Synergistic Pairs from the Inflammation Screen[a]

component 1	component 2	target 1	target 2	no. zHSA > 2
Cpd01	Cpd07	ADRB1	PDE4A	2
Cpd02	Cpd07	ADRB1	PDE4A	8
Cpd03	Cpd08	PDE4A	ADRB1	3
Cpd04	Cpd09	ADRB1	PDE4A	4
Cpd05	Cpd10	ADRB1	PDE4A	2
Cpd01	Cpd11	ADRB1	PDE4A	6
Cpd05	Cpd11	ADRB1	PDE4A	4
Cpd05	Cpd06	ADRB1	PDE4A	4
Cpd02	Cpd06	ADRB1	PDE4A	3
Cpd06	Cpd01	PDE4A	ADRB1	3
Cpd04	Cpd06	ADRB1	PDE4A	4

[a] Shown are compound IDs, the annotated target of the compounds, and the number of doses at which the ΔHSA was greater than 2 standard deviations from zero (criterion for significant synergism).

highest single activity.[14] We conclude that, to capture both potency shift and efficacy boost, one must use multiple synergy measures in the selection of active pairs (Figure 4d−f).

Traditional approaches to the discovery of synergistic combinations entail the rational design based on clinically congruent or complementary activities. The drawback of this approach is that it will miss the unexpected interactions within and between signaling pathways that are often seen in biological systems. While chemical space is vast, the number of well-validated tool compounds that merit testing in combinations is in the low thousands, a scale that is addressable by the proposed parsimonious synergy screening approach but not by previous techniques. Our results highlight the feasibility of efficiently and systematically screening for synergistic combinations provided the following criteria are met: the screening assay must be robust, the library must contain redundancy of activities, and the analysis must use multiple modes of synergism as hit criteria.

Although the scale of the presented 1027-compound screen is possible to contemplate as a simple all-pairs screen, the geometric scaling of combinations means that many simple questions are not addressable with the naïve approach. For example, a screen of pairwise combinations of three commercially available bioactive collections (Microsource Spectrum, Tocris Tocirscreen, Sigma LOPAC, ∼4400 compounds total) would entail $\sim 10^7$ assay points if pursued as a naïve pairwise screen (in singlicate). Our proposed method would reduce the well number to 4.8×10^5

dx.doi.org/10.1021/cb2003225 |*ACS Chem. Biol.* 2011, 6, 1391–1398

and would have the benefit of duplicate data. Thus a relatively straightforward question is brought from the inaccessible to the easily attainable.

In addition to pharmaceutical screening, the presented approach has the potential to significantly empower chemical genomics efforts. As has been seen with genetics, single node perturbations can be of utility in dissecting biology.[37] However, epistasis experiments have the ability to overcome redundancy, order members in pathways, and to identify crosstalk between pathways.[38−40] Similarly, in the case of chemical genomics, utilization of tool compounds one at a time will provide a relatively impoverished view of the biology in question, one that can be significantly broadened and enhanced with epistasis information.[41−44] The proposed method can be used to interrogate a much larger fraction of biological interactions, potentially limited only by assay and tool compound availability.

METHODS

Compound Libraries. For the viability screen, 11 targeted or broadly acting chemotherapeutic compounds were selected from the literature, and 89 compounds were selected from the Tocriscreen set (Tocris Bioscience) on the basis of structural diversity criteria and sample availability. For the inflammation screen, a set of 1027 bioactive compounds was selected from an internal proprietary collection. These compounds have known activities against a series of targets of interest to therapeutic groups.

Pool Design. Pool design begins with the shifted transversal design[45,46] to select pools of 10 compounds covering most pairs. However, this method does not yield complete coverage of the design space with equal-sized pools. Therefore, we recursively iterated the algorithm on the subsets of pairs that were not covered in the first pass to fill out the design. Finally, a small number of remaining deficiencies were filled with a greedy search. This approach was relatively efficient: all pairs of 1027 compounds were represented in 12,537 pools of 10, versus 11,708 ($_{1027}C_2/45$) for an optimal design. In addition to the pools, each compound was also tested as a single compound at 1 and 10 μM in triplicate. To create a self-deconvoluting design, the same design was used twice with the compound identifiers permuted. For the viability screen, 136 pools were required to cover the 4950 combinations of 100 compounds, and unambiguous deconvolution required repeating the design at least three times (four times was used in practice) with compound identities permuted.

Compound Management. The assay was performed using preplated compounds. Each individual compound was contained in a separate well of a 1536-well source plate (at a concentration of 2.8 mM in DMSO for the inflammation screen or 4 mM for the viability screen), and an acoustic dispenser was used to deliver 2.5 nL each of the mixture components to the appropriate well of the assay plates (for a final assay concentration of 1 μM in either 7 μL for the inflammation screen or 10 μL for the viability screen). Each assay well received 10 separate dispenses. For single-compound wells, DMSO was added to maintain a final volume of 25 nL. For dose−response experiments, serial dilutions were generated using a Biomek FX liquid handler (Beckman Coulter), plated in a 1536-well source plate, and an acoustic dispenser was used to combine the different doses of compounds.

Cell Culture. HCT116 (ATCC: CCL-247) colorectal carcinoma cells were maintained in McCoy's 5a medium, 10% FBS, penicillin/streptomycin at 37 °C and 5% CO_2. THP-1 monocytic cell line (ATCC: TIB-202) were grown in T-75 culture flasks in RPM 1640, 10% FBS, penicillin/streptomycin, and 50 μM 2-mercaptoethenol. Forty hours prior to experiments, cultures were harvested and seeded into fresh T-75 flasks at 3.5×10^5 cells mL^{-1} in 30 mL of growth medium and prestimulated with IFNγ at a final concentration of 40 ng mL^{-1}.

Viability Screen. Four hundred HCT116 cells in 10 μL of growth medium were added per well of the assay plate with compounds preplated. Control wells had only DMSO preplated, negative controls were seeded with cells, and positive control wells were seeded with cell-free medium. Seventy-two hours after plating, viability was assessed by adding 3.3 μL of 4x CellTiter Glo reagent (Promega), incubating for 10 min, and reading luminescence. Hit picking criteria were determined by exploration of the distribution and reproducibility of the synergy metrics, and a threshold was selected on the basis of the apparent signal *vs* noise boundary prior to pool deconvolution.

Inflammation Screen. Five thousand THP-1 cells per well were added to the assay plates with compounds preplated, followed by stimulation (lipopolysaccharide/interferon γ, 25 and 295 ng/mL final, respectively) after 1 h. IL6 HTRF (Cisbio) antibodies were also added to the culture. Twenty-four hours later, secreted IL6 was measured by adding KF to 400 mM and incubating 3 h at RT before reading fluorescence. Viability of THP-1 cells was assayed by removing media from a parallel culture to 5 μL (after the same 24 h stimulation) and adding 5 μL of 2x CellTiter Glo reagent, followed by a luminescence read. Controls for the screen were DMSO with or without stimulation (negative and positive controls, respectively, 44 each per plate, distributed throughout plate). Hit thresholds were determined *via* exploratory data analysis and prior to pool deconvolution, as for the HCT116 viability screen.

Liquid Handling. Compounds were dispensed with ATS-100 acoustic dispensers (EDC) into low-base, white (THP1) or black (HCT116), cell culture treated, polystyrene 1536-well plates (Aurora). Cell and stimulant dispenses were performed with a BioRapTR flying reagent dispenser (Beckman). HTRF reagent and CellTiter Glo were added to the assay plates using a BioRapTR, and luminescence and time-resolved fluorescence were read out using Envision or Viewlux readers (Perkin-Elmer). Media removal for the THP-1 viability assay was done with a GNF plate washer/dispenser.

Analysis. Data analysis was performed using Pipeline Pilot (versions 7 and 7.5, Accelrys), which in turn utilized R scripts[47] for calculations. Models for synergy based on Loewe additivity (combination index[10] and Bliss independence[21] were used in addition to a highest single activity (HSA) model.[14] In confirmation experiments where replicates were run, significance of synergy was assessed by calculating *z*-scores for replicate synergy metrics, and a threshold of $z > 2$ ($p \sim 0.05$) was selected for significance. Statistical tests were performed in the R environment,[47] and deconvolution (identifying recurring pairs in hit pools) was aided by the "arules" package.[48]

ASSOCIATED CONTENT

Supporting Information. This material is available free of charge via the Internet at http://pubs.acs.org.

AUTHOR INFORMATION

Corresponding Author

*E-mail: matthew_tudor@merck.com.

Present Addresses

[‡]Sanford-Burnham Medical Research Institute, Orlando, Florida 32827.

[§]NIH Chemical Genomic Center, National Human Genome Research Institute, National Institutes of Health, 9800 Medical Center Drive, Rockville, Maryland.

REFERENCES

(1) Keith, C. T., Borisy, A. A., and Stockwell, B. R. (2005) Multicomponent therapeutics for networked systems. *Nat. Rev.* 4, 71–78.

(2) Zimmermann, G. R., Lehar, J., and Keith, C. T. (2007) Multi-target therapeutics: when the whole is greater than the sum of the parts. *Drug Discovery Today 12*, 34–42.

(3) Arav-Boger, R., and Shapiro, T. A. (2005) Molecular mechanisms of resistance in antimalarial chemotherapy: the unmet challenge. *Ann. Rev. Pharmacol. Toxicol. 45*, 565–585.

(4) Vazquez, J. A. (2007) Combination antifungal therapy: the new frontier. *Fut. Microbiol. 2*, 115–139.

(5) Dancey, J. E., and Chen, H. X. (2006) Strategies for optimizing combinations of molecularly targeted anticancer agents. *Nat. Rev. 5*, 649–659.

(6) Dransfield, M. T., and Bailey, W. C. (2004) Fluticasone propionate/salmeterol for the treatment of chronic-obstructive pulmonary disease. *Expert Opin. Pharmacother. 5*, 1815–1826.

(7) Jeschke, M. G., Finnerty, C. C., Kulp, G. A., Przkora, R., Mlcak, R. P., and Herndon, D. N. (2008) Combination of recombinant human growth hormone and propranolol decreases hypermetabolism and inflammation in severely burned children. *Pediatr. Crit. Care Med. 9*, 209–216.

(8) Combates, N. J., Degiannis, D., Raskova, J., and Raska, K., Jr. (1995) Direct inhibition of human CD8+ lymphocyte activation by cyclosporine A and Rapamune-Sirolimus. *Clin. Immunol. Immunopathol. 77*, 221–228.

(9) Pascual, J. (2005) Concentration-controlled everolimus (Certican): combination with reduced dose calcineurin inhibitors. *Transplantation 79*, S76–79.

(10) Chou, T. C. (2006) Theoretical basis, experimental design, and computerized simulation of synergism and antagonism in drug combination studies. *Pharmacol. Rev. 58*, 621–681.

(11) Costa, F., and D'Elios, M. M. (2010) Management of *Helicobacter pylori* infection. *Expert Rev. Anti-Infect. Ther. 8*, 887–892.

(12) Bush, K., and Macielag, M. J. (2010) New beta-lactam antibiotics and beta-lactamase inhibitors. *Expert Opin. Ther. Pat. 20*, 1277–1293.

(13) Marcus, R., Paul, M., Elphick, H., and Leibovici, L. (2011) Clinical implications of beta-lactam-aminoglycoside synergism: systematic review of randomised trials. *Int. J. Antimicrob. Agents 37*, 491–503.

(14) Borisy, A. A., Elliott, P. J., Hurst, N. W., Lee, M. S., Lehar, J., Price, E. R., Serbedzija, G., Zimmermann, G. R., Foley, M. A., Stockwell, B. R., and Keith, C. T. (2003) Systematic discovery of multicomponent therapeutics. *Proc. Natl. Acad. Sci. U.S.A. 100*, 7977–7982.

(15) Chung, T. (1998) Screen compounds singly: Why muck it up. *J. Biomol. Screening 3*, 171–173.

(16) Ferrand, S., Schmid, A., Engeloch, C., and Glickman, J. F. (2005) Statistical evaluation of a self-deconvoluting matrix strategy for high-throughput screening of the CXCR3 receptor. *Assay Drug Dev. Technol. 3*, 413–424.

(17) Hodder, P., Mull, R., Cassaday, J., Berry, K., and Strulovici, B. (2004) Miniaturization of intracellular calcium functional assays to 1536-well plate format using a fluorometric imaging plate reader. *J. Biomol. Screening 9*, 417–426.

(18) Liu, Y., Lacson, R., Cassaday, J., Ross, D. A., Kreamer, A., Hudak, E., Peltier, R., McLaren, D., Munoz-Sanjuan, I., Santini, F., Strulovici, B., and Ferrer, M. (2009) Identification of small-molecule modulators of mouse SVZ progenitor cell proliferation and differentiation through high-throughput screening. *J. Biomol. Screening 14*, 319–329.

(19) Greco, W. R., Bravo, G., and Parsons, J. C. (1995) The search for synergy: a critical review from a response surface perspective. *Pharmacol. Rev. 47*, 331–385.

(20) Loewe, S. (1928) Die quantitativen Probleme der Pharmakologie. *Ergebn. Physiol. 27*, 47–187.

(21) Bliss, C. (1939) The toxicity of poisons applied jointly. *Ann. Appl. Biol. 26*, 585–615.

(22) Webb, J. (1963) Effect of more than one inhibitor, in *Enzymes and Metabolic Inhibitors*, Vol. 1, pp 487−512, Academic Press, New York.

(23) Engelman, J. A., Chen, L., Tan, X., Crosby, K., Guimaraes, A. R., Upadhyay, R., Maira, M., McNamara, K., Perera, S. A., Song, Y., Chirieac, L. R., Kaur, R., Lightbown, A., Simendinger, J., Li, T., Padera, R. F., Garcia-Echeverria, C., Weissleder, R., Mahmood, U., Cantley, L. C., and Wong, K. K. (2008) Effective use of PI3K and MEK inhibitors to treat mutant Kras G12D and PIK3CA H1047R murine lung cancers. *Nat. Med. 14*, 1351–1356.

(24) Sunayama, J., Matsuda, K., Sato, A., Tachibana, K., Suzuki, K., Narita, Y., Shibui, S., Sakurada, K., Kayama, T., Tomiyama, A., and Kitanaka, C. (2010) Crosstalk between the PI3K/mTOR and MEK/ERK pathways involved in the maintenance of self-renewal and tumorigenicity of glioblastoma stem-like cells. *Stem Cells 28*, 1930–1939.

(25) Balko, J. M., Jones, B. R., Coakley, V. L., and Black, E. P. (2009) Combined MEK and EGFR inhibition demonstrates synergistic activity in EGFR-dependent NSCLC. *Cancer Biol. Ther. 8*, 522−530.

(26) Ou, D. L., Shen, Y. C., Liang, J. D., Liou, J. Y., Yu, S. L., Fan, H. H., Wang, D. S., Lu, Y. S., Hsu, C., and Cheng, A. L. (2009) Induction of Bim expression contributes to the antitumor synergy between sorafenib and mitogen-activated protein kinase/extracellular signal-regulated kinase kinase inhibitor CI-1040 in hepatocellular carcinoma. *Clin. Cancer Res. 15*, 5820–5828.

(27) McCaig, A. M., Cosimo, E., Leach, M. T., and Michie, A. M. Dasatinib inhibits B cell receptor signalling in chronic lymphocytic leukaemia but novel combination approaches are required to overcome additional pro-survival microenvironmental signals. (2011) *Br. J. Haematol.* 153, 199−211. DOI: 10.1111/j.1365-2141.2010.08507.x.

(28) Zhang, J. H., Chung, T. D., and Oldenburg, K. R. (1999) A simple statistical parameter for use in evaluation and validation of high throughput screening assays. *J. Biomol. Screening 4*, 67–73.

(29) Cobelens, P. M., Kavelaars, A., Vroon, A., Ringeling, M., van der Zee, R., van Eden, W., and Heijnen, C. J. (2002) The beta 2-adrenergic agonist salbutamol potentiates oral induction of tolerance, suppressing adjuvant arthritis and antigen-specific immunity. *J. Immunol. 169*, 5028–5035.

(30) Kim, D. H., Muthyala, S., Soliven, B., Wiegmann, K., Wollmann, R., and Chelmicka-Schorr, E. (1994) The beta 2-adrenergic agonist terbutaline suppresses experimental allergic neuritis in Lewis rats. *J. Neuroimmunol. 51*, 177–183.

(31) Verhoeckx, K. C., Doornbos, R. P., van der Greef, J., Witkamp, R. F., and Rodenburg, R. J. (2005) Inhibitory effects of the beta-adrenergic receptor agonist zilpaterol on the LPS-induced production of TNF-alpha in vitro and in vivo. *J. Vet. Pharmacol. Ther. 28*, 531–537.

(32) Diamant, Z., and Spina, D. (2011) PDE4-inhibitors: A novel, targeted therapy for obstructive airways disease. *Pulm. Pharmacol. Ther. 24*, 353–360.

(33) Nials, A. T., Tralau-Stewart, C. J., Gascoigne, M. H., Ball, D. I., Ranshaw, L. E., and Knowles, R. G. (2011) In vivo characterisation of GSK256066, a high affinity inhaled phosphodiesterase 4 inhibitor. *J. Pharmacol. Exp. Ther. 337*, 137–144.

(34) Juergens, U. R., Stober, M., Libertus, H., Darlath, W., Gillissen, A., and Vetter, H. (2004) Different mechanisms of action of beta2-adrenergic receptor agonists: a comparison of reproterol, fenoterol and salbutamol on monocyte cyclic-AMP and leukotriene B4 production in vitro. *Eur. J. Med. Res. 9*, 365–370.

(35) Killian, U., Schudt, C. (2006) Altana Pharma AG, *Synergistic combination*, U.S. Patent 7056936.

(36) Teixeira, M. M., Rossi, A. G., Giembycz, M. A., and Hellewell, P. G. (1996) Effects of agents which elevate cyclic AMP on guinea-pig eosinophil homotypic aggregation. *Br. J. Pharmacol. 118*, 2099–2106.

(37) Giaever, G., Chu, A. M., Ni, L., Connelly, C., Riles, L., Veronneau, S., Dow, S., Lucau-Danila, A., Anderson, K., Andre, B., Arkin, A. P., Astromoff, A., El-Bakkoury, M., Bangham, R., Benito, R., Brachat, S., Campanaro, S., Curtiss, M., Davis, K., Deutschbauer, A., Entian, K. D., Flaherty, P., Foury, F., Garfinkel, D. J., Gerstein, M., Gotte, D., Guldener, U., Hegemann, J. H., Hempel, S., Herman, Z., Jaramillo, D. F., Kelly, D. E., Kelly, S. L., Kotter, P., LaBonte, D., Lamb, D. C., Lan, N., Liang, H., Liao, H., Liu, L., Luo, C., Lussier, M., Mao, R., Menard, P., Ooi, S. L., Revuelta, J. L., Roberts, C. J., Rose, M., Ross-Macdonald, P., Scherens, B., Schimmack, G., Shafer, B., Shoemaker, D. D., Sookhai-Mahadeo, S., Storms, R. K., Strathern, J. N., Valle, G., Voet, M., Volckaert, G., Wang,

C. Y., Ward, T. R., Wilhelmy, J., Winzeler, E. A., Yang, Y., Yen, G., Youngman, E., Yu, K., Bussey, H., Boeke, J. D., Snyder, M., Philippsen, P., Davis, R. W., and Johnston, M. (2002) Functional profiling of the *Saccharomyces cerevisiae* genome. *Nature 418*, 387–391.

(38) Costanzo, M., Baryshnikova, A., Bellay, J., Kim, Y., Spear, E. D., Sevier, C. S., Ding, H., Koh, J. L., Toufighi, K., Mostafavi, S., Prinz, J., St Onge, R. P., VanderSluis, B., Makhnevych, T., Vizeacoumar, F. J., Alizadeh, S., Bahr, S., Brost, R. L., Chen, Y., Cokol, M., Deshpande, R., Li, Z., Lin, Z. Y., Liang, W., Marback, M., Paw, J., San Luis, B. J., Shuteriqi, E., Tong, A. H., van Dyk, N., Wallace, I. M., Whitney, J. A., Weirauch, M. T., Zhong, G., Zhu, H., Houry, W. A., Brudno, M., Ragibizadeh, S., Papp, B., Pal, C., Roth, F. P., Giaever, G., Nislow, C., Troyanskaya, O. G., Bussey, H., Bader, G. D., Gingras, A. C., Morris, Q. D., Kim, P. M., Kaiser, C. A., Myers, C. L., Andrews, B. J., and Boone, C. (2010) The genetic landscape of a cell. *Science 327*, 425–431.

(39) Schuldiner, M., Collins, S. R., Thompson, N. J., Denic, V., Bhamidipati, A., Punna, T., Ihmels, J., Andrews, B., Boone, C., Greenblatt, J. F., Weissman, J. S., and Krogan, N. J. (2005) Exploration of the function and organization of the yeast early secretory pathway through an epistatic miniarray profile. *Cell 123*, 507–519.

(40) Tong, A. H., Lesage, G., Bader, G. D., Ding, H., Xu, H., Xin, X., Young, J., Berriz, G. F., Brost, R. L., Chang, M., Chen, Y., Cheng, X., Chua, G., Friesen, H., Goldberg, D. S., Haynes, J., Humphries, C., He, G., Hussein, S., Ke, L., Krogan, N., Li, Z., Levinson, J. N., Lu, H., Menard, P., Munyana, C., Parsons, A. B., Ryan, O., Tonikian, R., Roberts, T., Sdicu, A. M., Shapiro, J., Sheikh, B., Suter, B., Wong, S. L., Zhang, L. V., Zhu, H., Burd, C. G., Munro, S., Sander, C., Rine, J., Greenblatt, J., Peter, M., Bretscher, A., Bell, G., Roth, F. P., Brown, G. W., Andrews, B., Bussey, H., and Boone, C. (2004) Global mapping of the yeast genetic interaction network. *Science 303*, 808–813.

(41) Lehar, J., Krueger, A., Zimmermann, G., and Borisy, A. (2008) High-order combination effects and biological robustness. *Mol. Syst. Biol. 4*, 215.

(42) Lehar, J., Stockwell, B. R., Giaever, G., and Nislow, C. (2008) Combination chemical genetics. *Nat. Chem. Biol. 4*, 674–681.

(43) Lehar, J., Zimmermann, G. R., Krueger, A. S., Molnar, R. A., Ledell, J. T., Heilbut, A. M., Short, G. F., 3rd, Giusti, L. C., Nolan, G. P., Magid, O. A., Lee, M. S., Borisy, A. A., Stockwell, B. R., and Keith, C. T. (2007) Chemical combination effects predict connectivity in biological systems. *Mol. Syst. Biol. 3*, 80.

(44) Yeh, P., Tschumi, A. I., and Kishony, R. (2006) Functional classification of drugs by properties of their pairwise interactions. *Nat. Genet. 38*, 489–494.

(45) Kainkaryam, R. M., and Woolf, P. J. (2008) poolHiTS: a shifted transversal design based pooling strategy for high-throughput drug screening. *BMC bioinformatics 9*, 256.

(46) Thierry-Mieg, N. (2006) A new pooling strategy for high-throughput screening: the Shifted Transversal Design. *BMC Bioinformatics 7*, 28.

(47) R Development Core Team (2009) *R: A Language and Environment for Statistical Computing*, R Foundation for Statistical Computing, Vienna, Austria.

(48) Hahsler, M., Grun, B., and Hornik, K. (2005) arules—a computational environment for mining association rules and frequent item sets. *J. Stat. Software 14*, 1–25.